



Shale Petrophysics, Rock Physics and Geomechanics with Applications to the Indian Shale Prospects

Manika Prasad, Colorado School of Mines*

Analysis should be based on all available data to gain a geological interpretation of the reservoir.

Abstract

A major challenge in successful development of mudrock reservoirs, better known as shale plays, lies in determining the sweet spots for completion and in estimating the available resource. The parameters needed for resource development must be evaluated from rigorous rock physics and petrophysics analyses. These parameters are mostly obtained from rock physics and rock mechanics assessment of well log and laboratory data as well as petrophysical analysis. For example, understanding the elastic behavior of reservoir rocks can provide crucial information about the amount of generated hydrocarbon, petrophysical properties and geomechanical characteristics. Similarly, knowledge about the pore topology is required to model transport properties. The topology information is often obtained from microscopic images (SEM or CT images) or from pore size distribution measurements.

In this paper, rock physics, rock mechanics, and petrophysics analyses to study unconventional reservoirs, such as shales along with a few examples from tight sands are presented. Fundamentally, any analysis should honor all available data to gain a geologically realistic interpretation of reservoir rocks and seismic or hydraulic units.

Introduction

Understanding the elastic behavior of source rocks and its interrelation with organic content and maturity can provide crucial information about the amount of generated hydrocarbon, petrophysical properties and geomechanical characteristics from well logs and seismic surveys.

There are various assessment criteria for resource exploration, development, and completions strategy. In this paper, some of the key parameters and their evaluations status are discussed. Here, evaluations of the petrophysical parameter, porosity, and the effect of kerogen maturity on porosity determinations as well as its correlations with acoustic properties are presented. These two parameters, mostly obtained from rock physics and rock mechanics assessment of well log and laboratory data, allow us to evaluate shale reservoirs.

Pore topology information for modeling transport properties in shales is often obtained from microscopic images (SEM or CT images) or from pore size distribution measurements. Kuila and Prasad (2013a; 2013b) and Saidian et al. (2016a; 2016b) have shown the effects of fine grains, small pores, high clay content, swelling clay minerals and pores hosted in organic content on porosity measurements. The measured porosity and pore or throat size distribution using subcritical nitrogen (N₂) gas adsorption at 77.3 K, mercury intrusion (MI), water immersion (WI), and helium porosimetry based on Gas Research Institute standard methodology (GRI) showed significant differences based on the method used. A key understanding from such studies was that the method-dependent porosity measurements provided more information about the formations. Our intent is to provide a better understanding of the inconsistencies found in modeling transport properties in shales using laboratory measurements. An indiscriminate use of data without evaluating the experimental methods can lead to ambiguity.

Horizontal stresses in the subsurface are evaluated using well log information. Here, the acoustic logs are used to calculate the Young's modulus and Poisson's ratio. A case is presented, where adding the knowledge anisotropy to acoustic property data allows a more realistic estimate of horizontal stress from well logs. The horizontal stress field is critical during completions to predict fracture containment and to prevent unwanted loss of fracture energy in to surrounding formations.

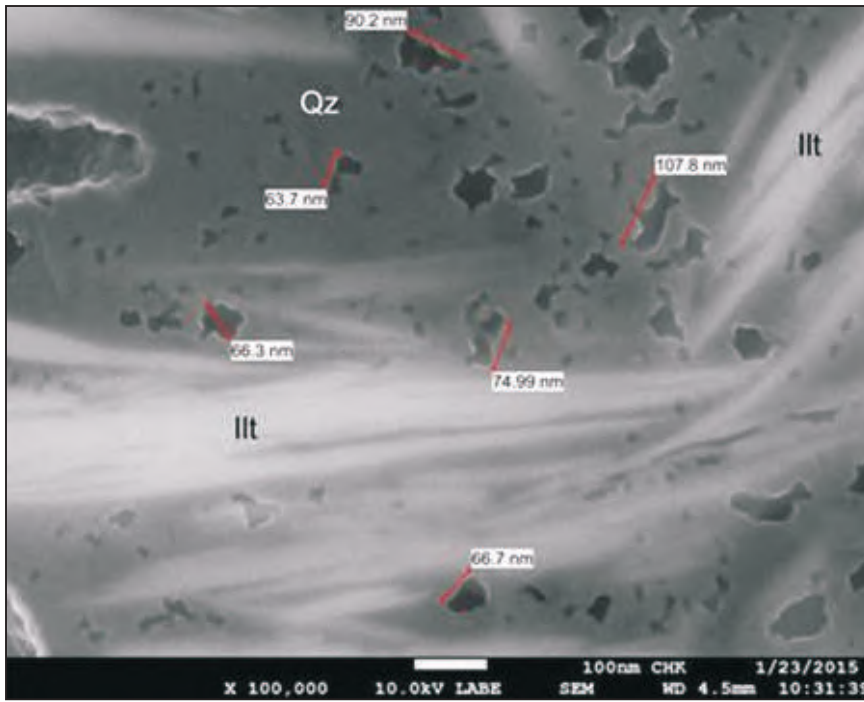
Pore Topology and Preferential Fluid Coverage

Pores in shale reservoirs are typically very small, often in the range of nanometers (Figure 1a, from Saidian et al., 2015a). In such small pores, the molecular sizes of the hydrocarbon and other fluids contained in the reservoirs play a large role. The pore network in shale reservoirs can act as molecular sieves to block or sorb fluid species. In Figure 1b, Milliken et al. (2013) show relative proportions of various gas molecules and their hypothetical distributions in pores hosted by organic matter that have pore diameters ranging several nanometers. Organic-matter hosted pores will preferentially contain methane and held closest to the pore wall. Table 1 shows a comparison between pore sizes, areas occupied by them and number of methane gas molecules hosted in the pores.

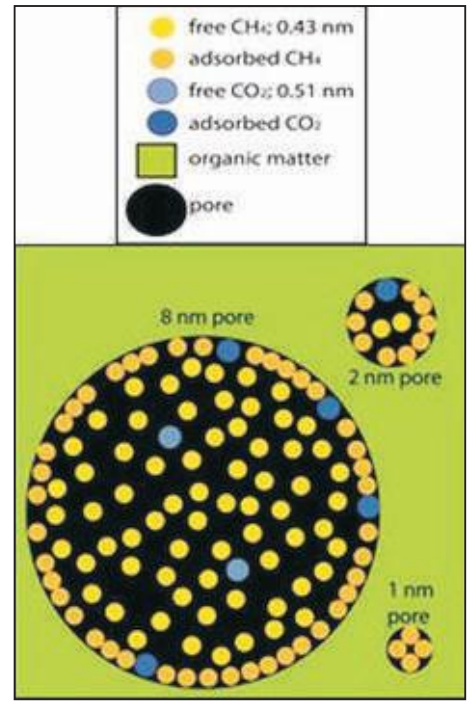
The implications here are that in gas shales, pores smaller than the detection limit by FE-SEM imaging will contain

Table 1: Pore size, its area and number of methane gas molecules it can contain using a methane molecule diameter of 0.43nm. Also, shown in the table are the number of methane molecules that would be adsorbed to the walls.

Pore (nm)	Area (nm ²)	Number of methane molecules in pore
1	0.79	4
2	3.14	11
8	50.27	130



a. from Saidian et al. (2016a).



b. From Milliken et al. (2013)

Fig. 1: Figure 1a shows an image of pore sizes in a typical Haynesville shale sample (from Saidian et al., 2016a). The numbers represent diameters of some of the larger pores. Figure 1b From Milliken et al. (2013) shows the relative sizes of gas molecules and OM-hosted pores. The relative sizes of methane and CO₂ gases are also presented. In the figure, adsorbed gas molecules are separated from free gas by a darker shade.

dominantly adsorbed gas. Diffusion flow could dominate the flow regime in such small pores. Free gas will mainly be contained in larger pores, primarily pores that are large enough to be imaged using, for example, FiB-SEM methods.

An added complication arises when, as in most cases, multiphase fluids are present in the pores. As shown in Figure 2, depending on their relative fluid mineral affinity, different fluids will preferentially cover separate regions in the rock. Figure 2 shows a typical mineral assemblage in a reservoir shale consisting of clay minerals, organic matter, and

silt grains. Pore fluids, methane and water, will separate with water in the clay mineral pores and methane in the organic pores (Williams, 2012).

Effect of Residual Fluid on Pore Space Measurements

Pore space quantification in shales depends on many factors. Numerous studies have shown that various factors lead to large errors in porosity measurements (Spears et al., 2011; Passey et al., 2012; Sondergeld et al., 2010; Kuila and Prasad, 2013a; Kuila and Prasad, 2013b; Saidian et al., 2016a; Saidian et al., 2016b). In a systematic analysis of porosity and surface area estimations, Zargari et al., (2015; 2016) showed that porosity and specific surface areas can be grossly underestimated in organic-rich shales. This discrepancy is particularly large in shales with maturity in the oil window. Figure 3 (from Zargari et al., 2015) shows pore size distributions measured in a series of Bakken shales with varying maturity. The measurements were made in the samples as received, and after successive cleaning with toluene, chloroform, and other solvents. As compared to original state, there are large changes in pore size distributions after washing with toluene and the other solvents. These changes indicate that a considerable volume of pores in organic-rich shales with maturity in the oil window remain filled with immovable hydrocarbons leading to lower estimates of their storage capacity. In cleaning the cores, the hydrocarbons that might still remain trapped in the shale are removed. These pores are available to the probing fluid and lead to higher measured porosity after cleaning. Note that the

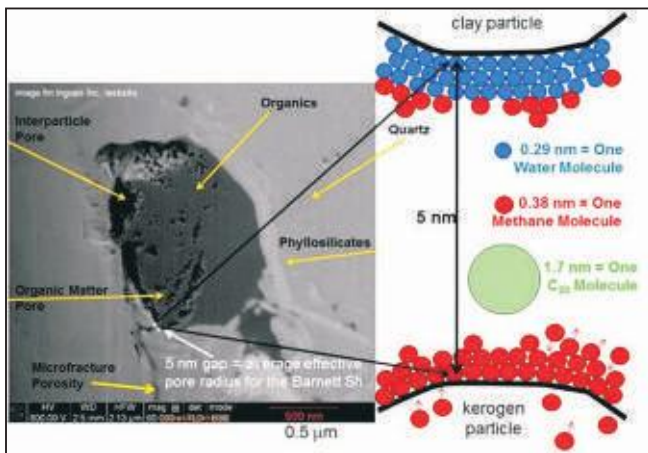


Fig. 2: Adapted from Williams(2012) showing preferential coverage depending on the affinity between the fluid and mineral substrate. Here, the water molecules preferentially adhere to clay minerals while the methane molecules attach to the organic surfaces.

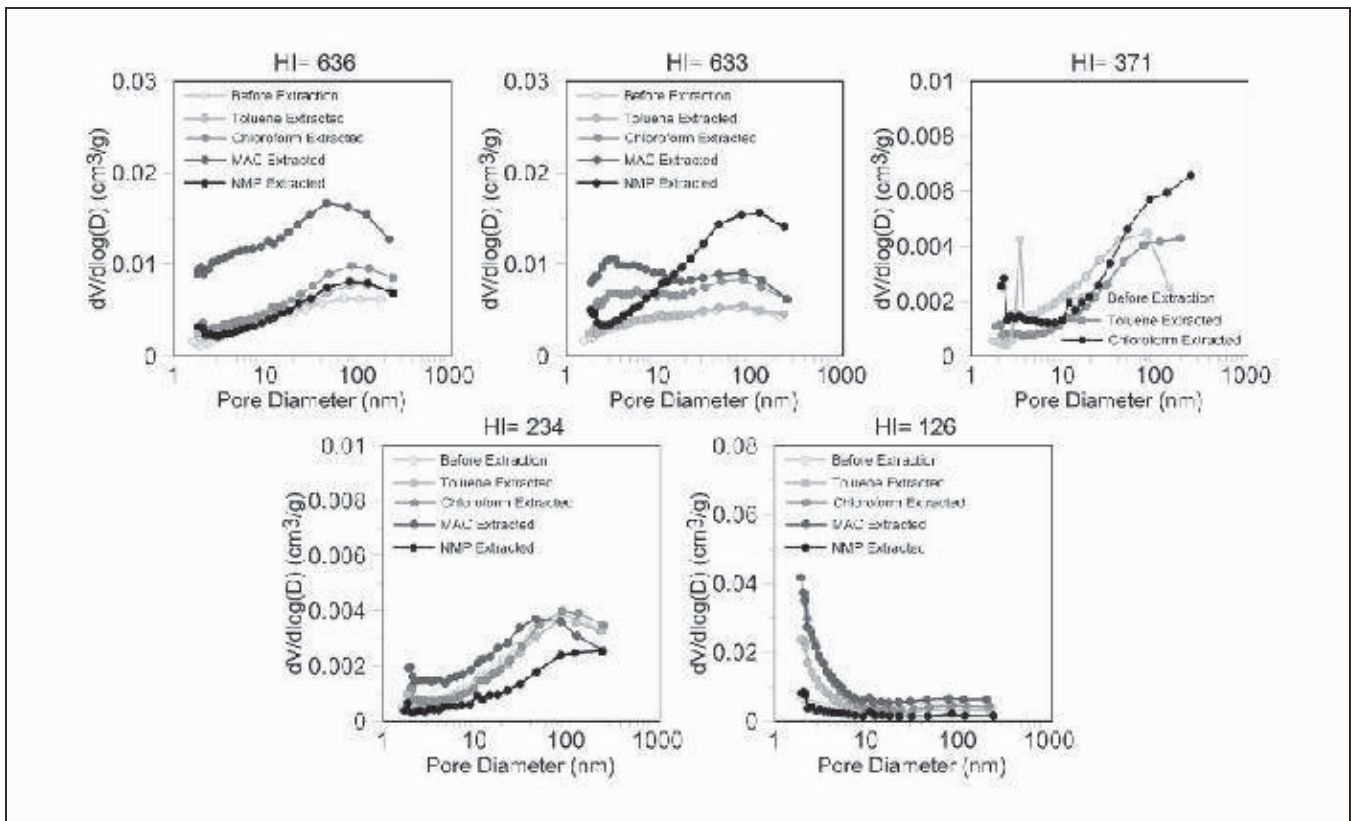


Fig. 3: Large changes in pore size distributions show that in organic-rich shales with maturity in the oil window, there is considerable presence of hydrocarbons. Thus, cleaning the cores will result in higher measured porosity due to removal of heavier hydrocarbons that might still remain trapped in the shale. This additional porosity will be dependent on the solvent used and on the maturity of the formation. (Figures from Zargari et al., 2015)

additional porosity will be dependent on the solvent used and on the maturity of the formation.

Changes in Acoustic Velocities

Acoustic velocity primarily shows an inverse correlation with porosity. However, as shown by Rivera and Prasad (2014), in addition to porosity, mineralogy also controls velocity. Figure 4 shows P-wave velocity plotted as a function of porosity for the porcelanites, dolomites and shales from the Monterey formation. The porcelanites and the shales lie on the same trend with porosity. However, the dolomitic rocks show slightly higher velocities. Corresponding to the velocities, NMR T2 relaxation data (Figure 5) show two distinct types of pore structures: while the dolomites show a broad bi-modal distribution of pore sizes. On the other hand, the porcelanites show a dominance of smaller pores. These small pores might also be an indication of fractures that would reduce velocities.

Systematic acoustic, petrophysical and flow property analysis allow a better understanding of the seismic, storage, and flow properties. They are also useful to build realistic rock physics models and to estimate the storage capacity or organic-rich shales. Acoustic properties also allow us to estimate in situ horizontal stresses. Figure 6 shows gamma ray and porosity logs from the Bakken formation. Upper Bakken shale and Lower Bakken shale are marked by very high GR values. Middle Bakken shows lower GR. It lies between Upper and Lower Bakken shales and is the target producing

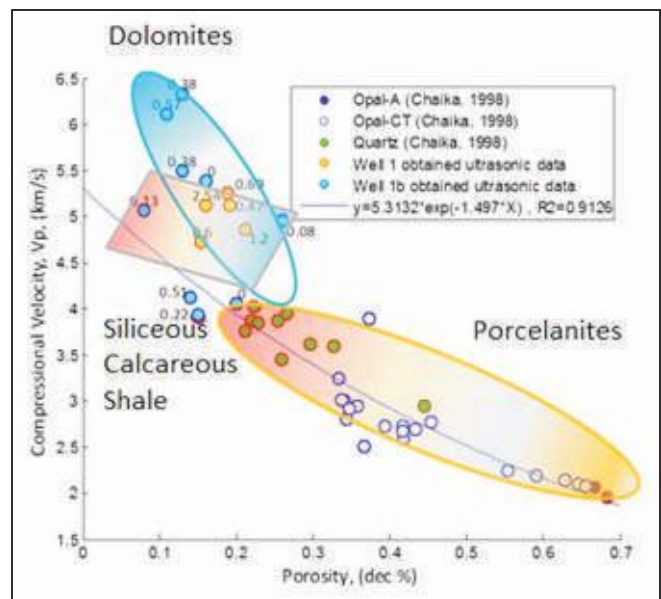
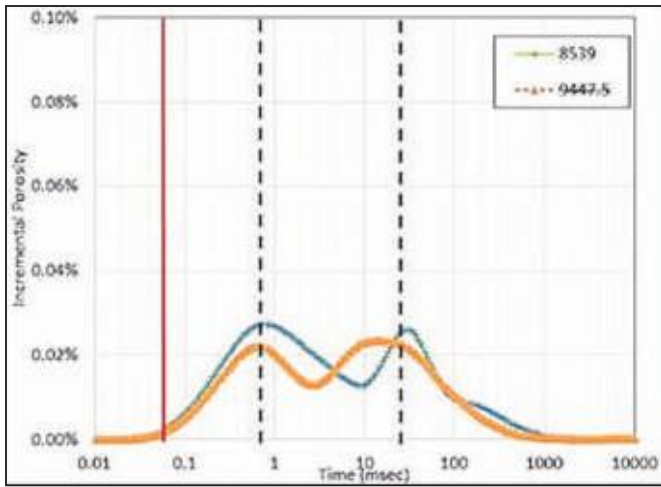
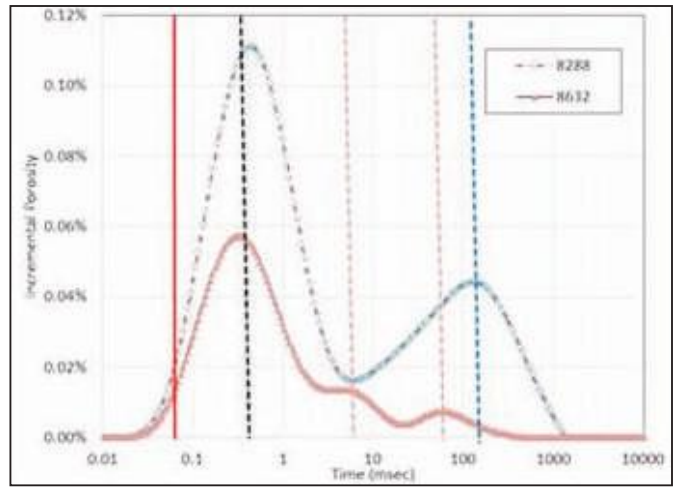


Fig. 4: Velocity porosity correlations in the Monterey shales, dolomites and porcelanites (modified from Rivera and Prasad, 2014).

formation. Since the target zone within Middle Bakken is often only 20 ft thick, the completion strategy must be carefully designed. One of the main criteria is the horizontal stress. A large stress contrast between the target and seal formations ensures that the induced fractures do not breach the



a. Dolomites



b. Porcelanites

Fig. 5: NMR T2 relaxations in the dolomites and porcelanites from the Monterey formation(modified from Rivera and Prasad, 2014). Figure 5a shows the broad bi-modal pore sizes in the dolomites with slightly larger relaxation times indicating presence of larger pores as compared to the porcelanites. Figure 5b shows NMR T2 relaxations in the porcelanites. Here the pores appear smaller with a predominance of the smaller pores over the larger ones. The vertical red line in both figures indicates instrument sensitivity limit.

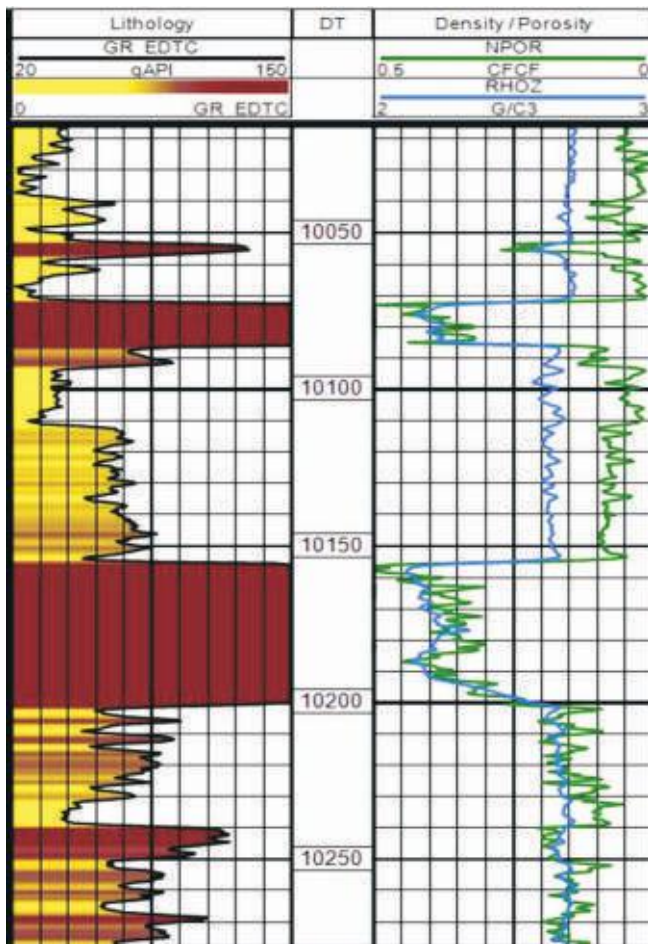


Fig. 6: Typical well log from the Bakken formation showing gamma ray log in the left track and porosity logs in the right track. The Upper Bakken shale lies between 10070 and 10090 ft while the Lower Bakken shale lies between 10155 and 10200 ft. Both shales are marked by high GR values. The Middle Bakken shows lower GR and lies between the Upper and Lower Bakken shales between 10090 and 10155 ft.

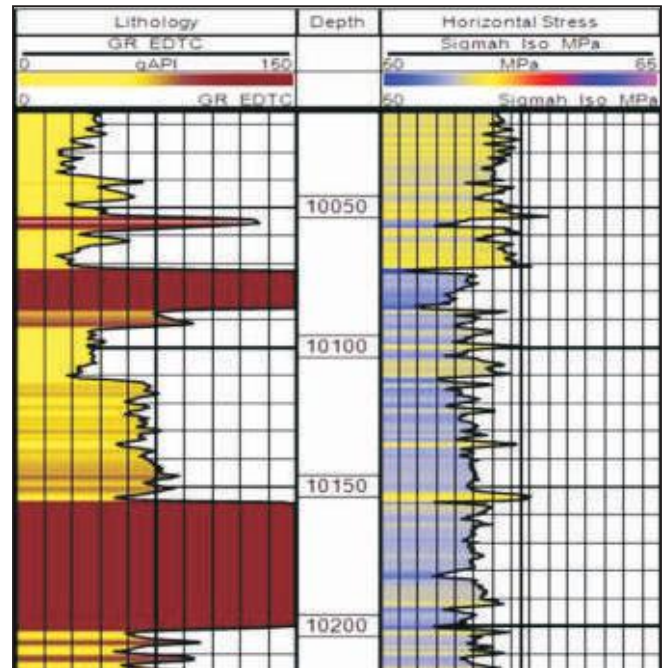


Fig. 7: Stress calculations using information from the Bakken formation well logs shown in Figure 6. The horizontal stress logs shown in the right track does not present much stress contrast between the Middle Bakken and the Upper and the Lower Bakken shales.

zone and fracture also adjacent zones. Such a breach would not only contaminate but also potentially loose fluids. Furthermore, the low stress contrast would waste valuable fracture energy in unwanted zones.

Horizontal stresses are often calculated from dipole sonic logs. Here the P- and S-wave velocity and the density logs are used to calculate Young's modulus and Poisson's ratio. Using these values, in Equation 1, the horizontal stress can be calculated.

$$(\sigma_h - \alpha \pi_p) = \frac{\nu}{1-\nu}(\sigma_v - \alpha \pi_p) + \text{Tectonic stress} \quad (1)$$

Here, σ denotes stresses with the subscript 'h' marking horizontal and 'v' marking vertical stresses; P_p denotes pore pressure; α is the Biot's effective stress coefficient; E is the Young's modulus; and ν is the Poisson's ratio.

ISOTROPIC CASE: Equation 1 describes the relations for isotropic cases. Thus, presuming tectonic stresses to be negligible and Biot coefficient ≈ 1 , the isotropic in situ stress equation yields almost constant horizontal stress throughout upper, middle, and lower Bakken (Figure 7). In such a scenario, fractures would not be contained in target Middle Bakken.

ANISOTROPIC CASE: Since the assumption of isotropy is not very realistic, it is necessary to calculate horizontal stresses for anisotropic formations. We first calculate the Biot's effective stress coefficient using the mineral modulus based on the formation lithology (K_{min}) and the bulk modulus (K) as shown in Equation 2.

$$\alpha = \left(1 - \frac{K}{K_{min}}\right) \quad (2)$$

Using Equation 2 to calculate Biot's effective stress coefficient for Bakken formation, the values for Biot's coefficient are shown in Figure 8.

In a simple scenario, honouring anisotropic texture and anisotropic velocities, horizontal stress can be calculated using Equation 3.

$$(\sigma_h - \alpha \pi_p) = \frac{E_h}{E_v} \frac{\nu_v}{1-\nu_h} (\sigma_v - \alpha \pi_p) + \text{Tectonic stress} \quad (3)$$

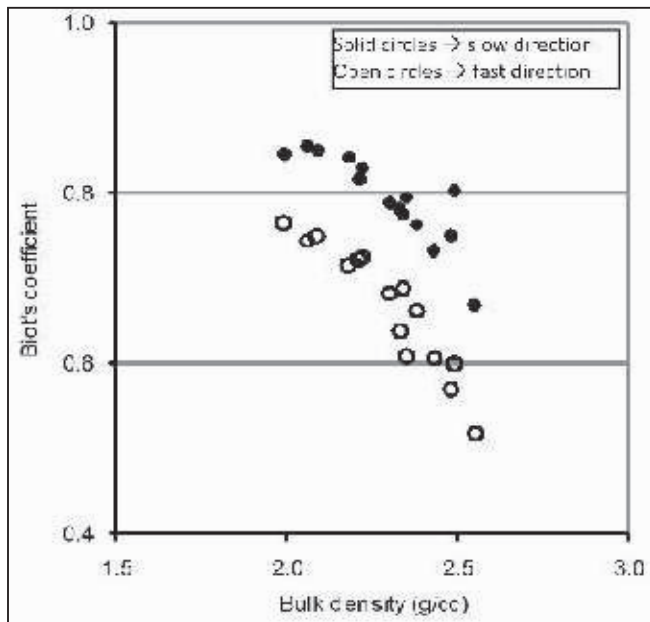


Fig. 8: Biot's coefficient calculated for Bakken formation shales (From Prasad et al., 2010). Note that the higher stiffness in the bedding parallel direction leads to lower Biot's coefficient in that direction.

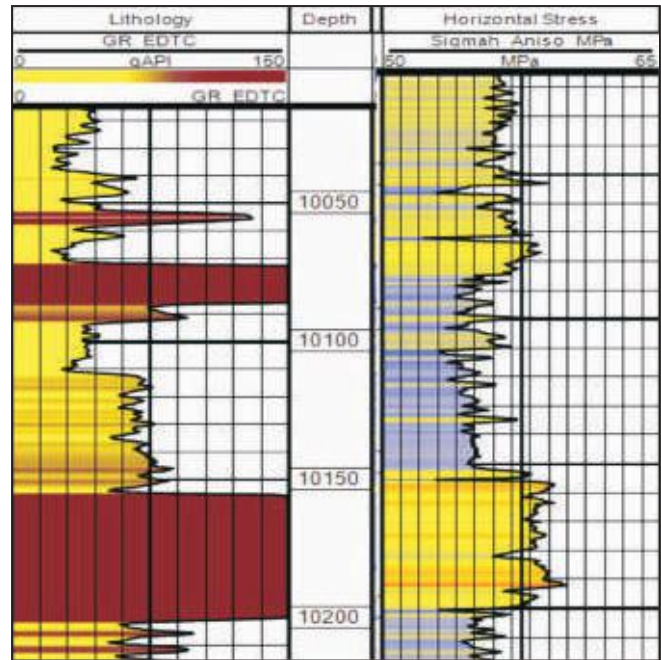


Fig. 9: Anisotropic horizontal stress calculations using information from the Bakken formation well logs shown in Figure 6. The horizontal stress logs shown in the right track now present a much larger stress contrast between the Middle Bakken and the Upper and the Lower Bakken shales.

Here, σ denotes stresses with the subscript 'h' marking horizontal and 'v' marking vertical stresses; P_p denotes pore pressure; α is Biot's effective stress coefficient; E is Young's modulus and ν is Poisson's ratio with the subscript 'h' marking bedding parallel and 'v' marking bedding-perpendicular directions. (Young's modulus: E_h horizontal, E_v vertical; Poisson's ratio: ν_h horizontal, ν_v vertical). The variation between E_v and E_h gives a different horizontal stress profile. Increased ν_h in the upper and lower Bakken imply that they will be more effective in hydrofracture containment.

References

- Kuila, U., Prasad, M., 2013a, Surface area and pore-size distribution in clays and shales: Geophysical Prospecting, 61, 341362.
- Kuila, U., Prasad, M., 2013b, Application of nitrogen gas-adsorption technique for characterization of pore structure of mudrocks: The Leading Edge, 32, #12, 14781485. doi: 10.1190/tle32121478.1
- Milliken, K. L., Rudnicki, M., Awwiller, D. N., & Zhang, T., 2013, Organic matter hosted pore system, Marcellus formation (Devonian), Pennsylvania: AAPG bulletin, 97, #2, 177-200.
- Passey, Q. R., Bohacs, K. M., Esch, W. L., Klimentidis, R., & Sinha, S., 2012, My source rock is now my reservoir: Geologic and petrophysical characterization of shale-gas reservoirs: AAPG Search and Discovery Article, 90124.
- Rivera, S., Prasad, M., 2014, Effect of Mineralogy on NMR, Sonic, and Resistivity: A Case Study of the Monterey Formation: Unconventional Resources Technology Conference, Denver, Colorado, 25-27 August 2014: pp. 68-87.
- Saidian, M., Kuila, U., Rivera, S., Godinez, L.J., and Prasad, M., 2016a, A Comparison of Measurement Techniques for Porosity and Pore Size Distribution in Shales (Mudrocks): A Case Study of Haynesville, Eastern European Silurian, Niobrara, and Monterey Formations: AAPG Memoir 112: Imaging Unconventional Reservoir Pore Systems, Pages 89-144, DOI: 10.1306/13592019M1123695

- Saidian, M., Godinez, L.J., Prasad, M., 2016b, Effect of clay and organic matter on nitrogen adsorption specific surface area and cation exchange capacity in shales (mudrocks): *Journal of Natural Gas Science and Engineering*, **33**, 1095-1106, doi:10.1016/j.jngse.2016.05.064.
- Sondergeld, C.H., Ambrose, R.J., Rai, C.S., and Moncrieff, J., 2010, Micro-Structural Studies of Gas Shales: Paper SPE 131771 presented at the SPE Unconventional Gas Conference, Pittsburg, Pennsylvania, USA, 23-25 February 2010. <http://dx.doi.org/10.2118/131771-MS>.
- Spears, R. W., Dudus, D., Foulds, A., Passey, Q., Esch, W. L., & Sinha, S., 2011, Shale gas core analysis: Strategies for normalizing between laboratories and a clear need for standard materials: presented at SPWLA 52nd Annual Logging Symposium. Society of Petrophysicists and Well-Log Analysts.
- Williams, K.E., 2012, The Permeability of Over pressure Shale Seals and of Source Rock Reservoirs is the Same: Search and Discovery Article #40935 presented at the AAPG 2012 Annual Convention and Exhibition, Long Beach, California, 22-25 April 2012.
- Zargari, S., Canter, L. C., Prasad, M., 2015, Porosity Evolution in Oil-prone Source Rocks: *Fuel* **153**, 110-117, doi:10.1016/j.fuel.2015.02.072
- Zargari*, S., Wilkinson*, T.M., Packard, C. E., Prasad, M., 2016, Effect of Thermal Maturity on Elastic Properties of Kerogen: *Geophysics*, **81**, 5, E297-E309.